Journal of Analytical and Applied Pyrolysis 157 (2021) 105219

Contents lists available at ScienceDirect

Journal of Analytical and Applied Pyrolysis

journal homepage: www.elsevier.com/locate/jaap

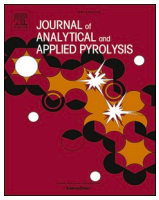

Bio-oil stability through stepwise pyrolysis of groundnut shells: Role of chemical composition, alkali and alkaline earth metals, and storage conditions

Anubhuti Bhatnagar *, Robert Barthen, Henrik Tolvanen, Jukka Konttinen

Tampere University, Korkeakoulunkatu 7, Tampere, 33720, Finland

ARTICLE INFO

Keywords:
Agro-residue
Slow pyrolysis
Accelerated aging
Bio-oil stability
Inorganic distribution

ABSTRACT

Bio-oil obtained from crop residues is unstable because of multiple reactive oxygenated compounds and alkali and alkaline earth metals (AAEMs), which hinder its use as a chemical feedstock. In the current study, stepwise pyrolysis of groundnut shells was performed in three-step (160/200–320/340–600 °C), two-step (320/340–600 °C), and continuous (600 °C) heating regimes to obtain a more stable bio-oil. The stability of bio-oils was compared in terms of changes to their pH, water content, AAEM concentration, and chemical composition over a fixed period. During three-step pyrolysis, 94.85–97.38 % of chemicals (anhydrosugars, organic acids, aldehydes, and ketones) were concentrated in step 2. In contrast, for two-step pyrolysis, 93.14–94.78 % were concentrated in step 1. The AAEMs transferred from groundnut shells to bio-oil were 7.04–9.63 % for three-step, 6.68–11.26 % for two-step, and 11.87 % for continuous pyrolysis. An accelerated aging test (80 °C for 24 h) showed that two-step pyrolysis at 340 °C and 600 °C, produced the most stable bio-oil despite a higher concentration of AAEMs. Further improvement in this bio-oil's stability was explored by altering storage temperature and adding solvents to the bio-oil. The decrease in concentrations of anhydrosugars and phenolics was <1% after four weeks of storage at 4 °C with the addition of methanol. The obtained results contribute to implementing stepwise pyrolysis units for crop residue management.

1. Introduction

Crop residues can be used as a lignocellulosic feedstock for biorefineries to produce chemicals such as organic acids, furfural, vanillin, levoglucosan, and liquid transportation fuels ethanol and methanol [1,2]. However, these residues are burnt in open fields [3] because of several issues, including low economic returns in collecting and transporting residues for centralized treatment [4,5] and a limited time window for sowing successive crops [6]. Groundnut shells (GNS) are an abundant resource for biorefineries, making up 20 % of the peanut pod. Current applications include a low heating-value energy source and manufacturing cardboard and pulp [7]. Pyrolysis has effectively converted crop residues, including GNS, into value-added products like adhesives, chemicals, and activated carbon [8,9]. Pyrolysis is the process of thermal decomposition and devolatilization of biomass between 400 °C and 700 °C in the absence of oxygen. The released volatiles are cooled to produce bio-oil, which is a mixture of water and chemicals such as esters, ethers, aldehydes, ketones, phenols, organic acids, and alcohols. These chemicals are highly reactive and alter the physical and chemical properties of bio-oil with time. This process is called 'aging' [10,11]. The reactions involved in aging are (1) esterification of organic acids, (2) the conversion of aldehydes to hydrates, hemiacetals, acetals, oligomers, or resins, (3) the conversion of unsaturated compounds to polyolefins and (4) the formation of acids and reactive chemical species due to oxidation by atmospheric oxygen [12]. These reactions may significantly alter the bio-oil composition and take a few weeks to stabilize [13,14].

The concentration of these reactive chemicals in the bio-oil depends on the nature of crop residues (water, ash, carbohydrate, and lignin content) and pyrolysis conditions (temperature, heating rate, and reactor type) [15]. Typically, crop residues can have 2–20 % ash content [15]. The alkaline and alkaline earth metals (AAEMs) in the ash catalyze dehydration and condensation reactions in the bio-oil vapors. These reactions decrease bio-oil heating value because of an increase in its water content (up to 25 %). This leads to the separation of an aqueous phase rich in polar compounds and a non-aqueous phase rich in

* Corresponding author.
E-mail address: anubhutibhatnagar@tuni.fi (A. Bhatnagar).

https://doi.org/10.1016/j.jaap.2021.105219
Received 18 January 2021; Received in revised form 17 May 2021; Accepted 25 May 2021
Available online 28 May 2021

non-polar and high-molecular-weight compounds [16]. AAEMs also promote the formation of pyrolysis gases and biochar over bio-oil [17], increase bio-oil viscosity over time, and act as catalyst poisons during the upgrading of bio-oil, causing corrosion in reactor equipment [18]. Although AAEMs largely remain sequestered in biochar, several mechanisms have been reported to explain their transfer to the bio-oil. These include the entrainment of char particles in bio-oil [18], the reaction of free radicals formed in the bio-oil vapors with the char-AAEM matrix [19,20], and the reaction of elements with carboxylate ions in the bio-oil vapors [21]. The entrainment of char in bio-oil occurs commonly in fluidized bed reactors. However, it has also been observed in the fixed bed reactors [21,22]. The transfer of AAEMs to bio-oil is governed by applying a continuous gas flow in the reactor. It can vary from <1% to 20 % [21,22]. In the absence of a continuous flow, there are secondary interactions between bio-oil vapors and the char-AAEM matrix, which creates a repeated release, diffusion, and adsorption of AAEMs from the char back into the fixed bed [21].

Stepwise heating could reduce bio-oil complexity, thus slowing down aging and improving bio-oil stability. Stepwise pyrolysis is based on the thermochemical stability of hemicellulose, cellulose, and lignin components present in the biomass. Stepwise pyrolysis involves heating biomass in discrete temperature steps to ensure a gradual release of the volatiles collected as separate fractions [23,24]. Two-step pyrolysis has been effectively used for crop residues such as groundnut shells, empty fruit bunch, and rice straw to concentrate carboxyl compounds, anhydrosugars, and carbonyl compounds in the first step and the unbranched phenolic compounds in the second step [25]. Stepwise heating is also expected to transfer AAEMs into different bio-oil fractions. However, because the thermal degradation of biomass components is not a discrete process, the selection of temperature and number of steps greatly influences the yield and bio-oil chemical composition [24].

The bio-oil obtained after stepwise heating can be further stabilized by adding solvents, such as low-molecular-weight alcohols, and reducing storage temperature [26,27]. Cordella et al. reported that up to 25 % of methanol was required to arrest the aging of the aqueous fraction of bio-oil [13]. Ren et al. reported that separating the aqueous and non-aqueous phases of the bio-oil derived by adding water improved the stability of both fractions [28]. Increasing bio-oil pH for enhancing the stability of certain reactive compounds such as anhydrosugars has been evaluated by [29]. Because solvent addition is a quick and effective method to slow down aging reactions, it can be of practical importance to store bio-oil. A list of recent research publications exploring aging mechanisms has been provided in the supplementary information (Table S1). These studies show that pyrolysis conditions, storage temperature, and pH affect the extent of aging reactions and distribution of AAEMs in bio-oil. There is a need to evaluate bio-oil stability in detail because these could reduce the concentration of desirable chemicals in bio-oil and hinder further chemical separations.

The authors found limited literature on studies that focus on the stability of bio-oil derived from high-ash crop residues using stepwise pyrolysis and studies that measure the degree of transfer of AAEMs into the bio-oil during pyrolysis. Thus, improving bio-oil stability using stepwise pyrolysis under different storage conditions may offer clear and coherent strategies for bio-oil applications. Further, the choice of pyrolysis temperature and storage conditions may depend on the bio-oil-derived chemicals because all storage conditions add to the process's economy. Hence, in the current study, we evaluate the most effective temperature steps for separating reactive chemicals and minimizing the transfer of AAEMs into the obtained bio-oil fractions obtained. The composition and storage stability of these bio-oil fractions were compared with bio-oil produced in a single step. Further, the role of storage temperature, solvents, and bio-oil pH in improving bio-oil storage stability was evaluated.

2. Materials and methods

2.1. Biomass characterization

For the current study, groundnut shell (GNS) was obtained from agro-industries in Tamil Nadu, India. Proximate analysis was performed using ASTM standards for moisture (ASTM E1358), volatiles (ASTM E872), and ash (ASTM E1755) content; fixed carbon was obtained by difference. The biomass composition is shown in Table 1, and except for moisture content, all other values are reported on a dry basis.

Biomass samples (0.5 g) were dried in the oven (105 °C overnight) and ground to a particle size of 200 μm before analysis. A Thermo Scientific™ Flash Smart™ Elemental Analyzer with a thermal conductivity detector was used to obtain the CHNS/O distribution. The distribution of AAEMs, Na, Mg, K, and Ca was analyzed by inductively coupled plasma mass spectrometry (ICP-MS, Thermo Scientific™, iCAP™ RQ). Dried biomass was incinerated at 600 °C for 2 h to obtain ash, which was digested with 10 mL of ultrapure concentrated HNO_3 (65 % solution) and 1 mL HF (38 % solution). Clear solutions were obtained after digestion. The final solution was diluted to 50 mL using ultrapure water and filtered (pore size 0.45 μm) before analysis. Further details about the sample preparation were reported in detail previously [25].

2.2. Pyrolysis experimental set-up

The pyrolysis reactor used in the current study has been described in detail previously [25]. The pyrolysis experimental set-up consisted of a stainless-steel reactor, and the reactor lid was sealed with a graphite gasket and dense screw fastening. Nitrogen gas (flowrate: 20 $Lmin^{-1}$) was used to purge the reactor of oxygen/ air before the heating started. The gas flow was maintained throughout the pyrolysis process until the reactor was cooled back to <100 °C. Pyrolysis was performed by adding 500 g of GNS (as received). The volatiles released during pyrolysis were passed through a water-cooled condenser. Bio-oil was collected in a glass bottle, and the gases were passed through the exhaust. The char formed during the reaction was collected and weighed after each batch.

The choice of temperature steps for pyrolysis was made by thermogravimetric analysis (TGA) using Linseis Simultaneous TGA (PT1600) and discussed in detail previously [25]. Oven-dried GNS (20 mg) was heated to 600 °C at 5 °C min^{-1} with nitrogen as a purge gas (flow rate: 200 mL min^{-1}). Fig. 1 shows the TGA and differential thermogravimetric (DTG) curves for thermal degradation of GNS.

The release of volatiles from biomass was linked with the rate of thermal degradation of its components [15]. Thermal degradation of GNS started at T_{onset} (157 °C). The incomplete peak marked as T_{HC} (207 °C) indicates the temperature at which hemicellulose and cellulose degradation temperatures overlapped. The point marked as T_{peak} (302 °C) indicates the temperature at which the cellulose breakdown

Table 1
Composition of groundnut shell (standard deviation in parenthesis).

Proximate analysis (as received, wt%)		
Moisture	6.62 (0.14)	
Volatiles	66.76 (1.64)	
Ash	4.61 (0.51)	
Fixed carbon (by difference)	22.01 (1.72)	
Elemental analysis (wt%)		
Element	Dry basis	Dry Ash Free Basis
Carbon	51.13 (0.15)	50.05 (0.15)
Hydrogen	6.29 (0.03)	6.15 (0.03)
Nitrogen	1.10 (0.02)	1.08 (0.02)
Sulfur	0.03 (0.01)	0.03 (0.01)
Oxygen (by difference)	41.45 (0.06)	42.69 (0.06)
Alkali and alkaline earth metals distribution (g/kg of dry feedstock)		
Na	8.87 (1.03)	
K	14.64 (0.13)	
Mg	2.47 (0.54)	
Ca	9.26 (0.53)	

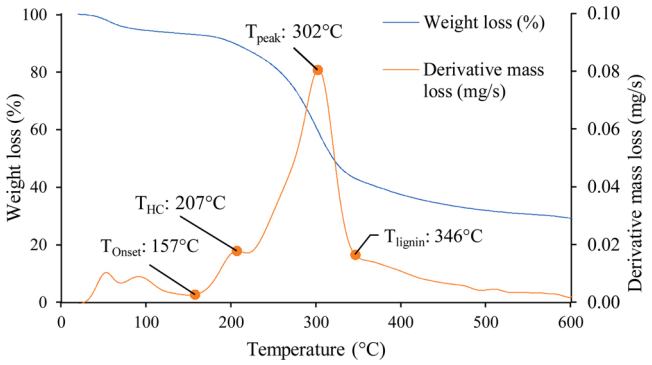

Fig. 1. Thermal behavior of groundnut shell observed in TGA [25].

rate was the highest. Beyond the point marked as T_{lignin} (346 °C), the remaining mass was attributed to the slow devolatilization of lignin which continues till 600 °C. These data points, three-step, two-step, and continuous pyrolysis temperatures, were set as shown in Table 2.

The heating rate was maintained at 5 °C min^{-1} during pyrolysis and was manually held at each temperature step for 15 min to collect the bio-oil fractions. The yields ($y_{product}$) of the biochar and bio-oil were obtained by Equation 1. The yield of the pyrolysis gases (y_{gas}) was calculated using Eq. 2.

$$y_{product}\ (wt.\%) = \left(\frac{weight_{product} * 100}{weight_{biomass}}\right) \quad (1)$$

$$\mathbf{y_{gas}}\ (\mathbf{wt.}\%) = 100 - \mathbf{y_{char}} - \mathbf{y_{bio-oil}} \quad (2)$$

$weight_{product}$ is the weight (in grams) of the char or bio-oil fractions collected from pyrolysis. $weight_{biomass}$ is the initial weight (in grams) of the biomass sample. Three identical pyrolysis tests using a bench-scale reactor were conducted, and the results are reported in Fig. 2.

2.3. Bio-oil characterization method

As the bio-oil vapors condensed, an aqueous and non-aqueous phase was formed in the collection bottle. The bio-oil aqueous phase was decanted from the top and filtered (pore size 0.45 μm). The mass yields of the aqueous (AqBO) and non-aqueous (NaqBO) fractions of bio-oil obtained from each temperature step during pyrolysis were recorded by weighing the filtrate and residue.

2.3.1. Physical and chemical composition of bio-oil

The water content of the bio-oil fractions was measured by Karl Fisher titration using Hydranal titrant and Hydranal solvent. A Metrohm 780 pH Meter was used to measure the pH of bio-oil fractions. AqBO and NaqBO's chemical composition were analyzed individually. An Agilent series 6890 Gas Chromatograph (GC), equipped with an HP-5MS capillary column (30 m, 0.25 mm ID, 0.25 μm film thickness) and helium as carrier gas (flow rate: 1 mL min^{-1}) was used for analysis. NaqBO samples were diluted with dichloromethane (DCM) in a 1:100 ratio, and AqBO samples were diluted with methanol in a 1:50 ratio. The inlet temperature was 250 °C, and the split ratio was 1:20. The column temperature was held at 40 °C for 5 min and then ramped up to 180 °C at 40 °C min^{-1} and held there for 13 min. Compounds were detected using an Agilent 5975B mass spectrometry (MS) detector and identified using the NIST Mass Spectral Library (NIST 05). The spectral information from the GCMS analysis of the bio-oil fractions is given in Figures S1-S5. Carboxyl compounds and anhydrosugars were detected in AqBO samples using Shimadzu (SIL-20 series) High Performance Liquid Chromatography (HPLC) equipped with a Rezex™ RHM-Monosaccharide H^+ (300 × 7.8 mm) column and a refractive index detector (RID-10 A). The column temperature was 70 °C, injection volume of 10 μL and the eluent was 10 mM of sulfuric acid (flow rate: 0.5 mL min^{-1}). The samples were diluted with ultrapure water in a 1:50 ratio before starting the analysis.

Amongst the chemicals detected, the nine most abundant chemicals in the bio-oil were quantified. These were acetic acid, levoglucosan, furfural, butyrolactone, 2-Hydroxy-3-methyl-2-cyclopenten-1-one (cyclotene), phenol, 2-Methoxyphenol (guaiacol), 2-Methoxy-4-methylphenol (p-methyl guaiacol) and 2-Methoxy-4-ethylphenol (p-ethyl guaiacol). The chemicals were grouped according to their functional groups for ease of comparison. Acetic acid was used as a marker for the carboxyl group. Levoglucosan was used as a marker for anhydrosugars. Furfural, butyrolactone, and cyclotene were grouped as carbonyls. Phenol, guaiacol, p-methyl guaiacol, p-ethyl guaiacol, and isoeugenol were grouped as phenolics. The concentration of all quantified chemicals quantified is given in Table 3. The separation efficiency (%) of the chemicals in each temperature step was estimated using Eq. 3.

$$\text{Separation efficiency}\ (\%) = \frac{(C_{i,\ AqBO} x\ m_{AqBO} + C_{i,\ NaqBO} x\ m_{NaqBO})_j}{\sum_{j=1}^{3}(C_{i,\ AqBO} x\ m_{AqBO} + C_{i,\ NaqBO} x\ m_{NaqBO})} \times 100 \quad (3)$$

where, C_i is the concentration of the chemical in AqBO or NaqBO (in mg/kg bio-oil), $m_{AqBO\ or\ NaqBO}$ is the mass fraction of bio-oil (kg/kg biomass), and j is the temperature step for pyrolysis from 1 to 3

2.3.2. Distribution of AAEMs

The distribution of AAEMs, Na, K, Mg, and Ca in the biochar and bio-oil was analyzed by ICP-MS. Biochar samples were prepared for analysis using the same method as described in Section 2.1. The bio-oil samples (fresh and aged) were digested with 10 mL of ultrapure concentrated HNO_3 (65 % solution) before analysis. Clear solutions were obtained after digestion. The final solution was diluted to 50 mL with ultrapure water and filtered (pore size 0.45 μm) before analysis. The degree of transfer (%) of AAEMs from GNS to bio-oil and biochar was estimated by Eq. 4. The mass balance over the distribution of AAEMs was measured by Eq. 5, assuming no elements were lost to pyrolysis gases.

$$\text{Degree of transfer}\ (\%) = \frac{(\alpha_{i,\ AqBO,\ NaqBO\ or\ Char})_j}{\alpha_{i,biomass}} \times 100 \quad (4)$$

$$\text{Mass balance}\ (\%) = \alpha_{i,\ AqBO} + \alpha_{i,\ NaqBO} + \alpha_{i,\ Char} \quad (5)$$

where, α_i (-) is the concentration of AAEM in biomass and pyrolysis products, and j is the pyrolysis step between 1 and 3.

2.4. Bio-oil stability assessment method

The storage stability of the obtained bio-oil fractions was assessed by evaluating the bio-oil composition change using accelerated aging, which involved storing bio-oil at 80 °C for 24 h. This method was used because the changes occurring at these conditions were equivalent to bio-oil changes that would occur over a long period, such as one to three years at a storage temperature of 20 °C [30,31]. The assessment was made for bio-oil fractions, which contained the highest concentration of all quantified chemicals (Table 3). AqBO obtained from step 2 in 3St-160−320 and 3St-200−340, from step 1 in 2St-320 and 2St-340, and

Table 2
Temperature steps for pyrolysis of biomass.

No. of steps	Identifier (No. of steps-Temp1-Temp2)	Step 1 Temperature (°C)	Step 2	Step 3
Three-step	3St-160−320	160	320	600
Three-step	3St-200−340	200	340	600
Two-step	2St-320	—	320	600
Two-step	2St-340	—	340	600
Continuous	Cont-600	—	—	600

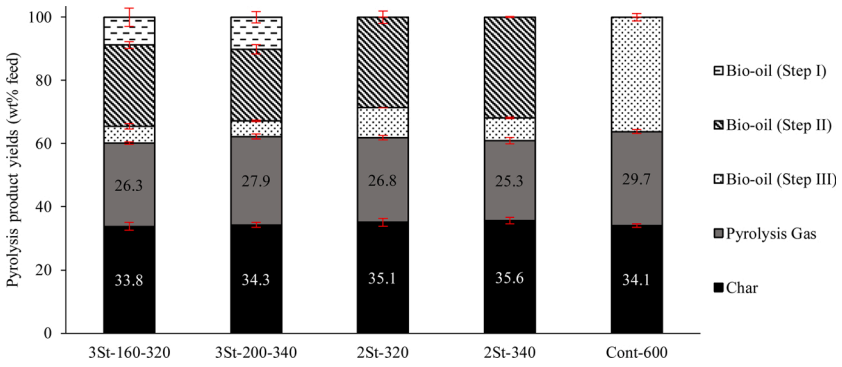

Fig. 2. Mass yields from stepwise and continuous pyrolysis of GNS.

Table 3
pH, water content (%) and concentration of chemicals (mg/kg biomass) in bio-oil from all pyrolysis cases (standard deviations in parenthesis; N.D. Not detected).

mg/kg biomass	3St-160−320			3St-200−340			2St-320		2St-340		Cont-600
	160 °C	320 °C	600 °C	200 °C	340 °C	600 °C	320 °C	600 °C	340 °C	600 °C	600 °C
Water (% in BO)	80.99 (1.70)	51.82 (0.74)	72.09 (1.42)	82.41 (1.27)	52.87 (0.83)	79.53 (0.84)	67.87 (1.75)	79.57 (0.65)	62.16 (1.00)	84.39 (1.10)	69.70 (0.85)
pH	3.56 (0.02)	3.60 (0.01)	7.87 (0.02)	3.86 (0.03)	3.70 (0.01)	9.07 (0.02)	3.55 (0.01)	8.53 (0.02)	3.65 (0.02)	8.56 (0.03)	4.23 (0.02)
Acetic acid	46.28 (19.91)	3166.52 (38.10)	201.97 (2.17)	123.99 (30.93)	3053.24 (162.08)	66.05 (5.64)	2879.97 (163.78)	131.64 (10.54)	3090.95 (110.77)	292.47 (0.92)	4924.14 (747.28)
Levoglucosan	29.60 (1.73)	1551.74 (116.80)	36.08 (2.55)	35.39 (14.01)	1499.85 (46.86)	14.07 (7.16)	1009.33 (8.80)	59.96 (1.68)	1773.18 (123.31)	77.66 (1.12)	1936.75 (260.63)
Furfural	37.32 (2.14)	762.24 (89.40)	14.95 (2.35)	207.81 (76.54)	836.62 (1.01)	14.68 (1.72)	765.16 (32.14)	53.34 (1.27)	702.51 (19.15)	89.44 (1.12)	902.22 (40.10)
Butyrolactone	N.D.	897.26 (83.98)	29.48 (12.99)	53.02 (0.27)	959.94 (73.02)	21.39 (0.46)	774.66 (3.84)	63.33 (9.14)	969.54 (45.96)	120.08 (0.36)	922.98 (43.98)
Cyclotene	N.D.	395.00 (3.04)	9.90 (0.05)	14.32 (0.01)	391.13 (10.27)	5.18 (0.26)	512.29 (7.35)	39.55 (0.71)	464.07 (5.33)	N.D.	639.11 (15.47)
Phenol	N.D.	1005.39 (57.26)	50.70 (8.51)	36.95 (0.01)	892.91 (114.92)	46.65 (17.00)	992.66 (7.91)	76.66 (0.47)	923.61 (17.33)	58.90 (4.85)	1227.05 (12.86)
Guaiacol	N.D.	773.81 (28.26)	16.58 (4.19)	26.60 (0.51)	979.72 (47.58)	13.32 (1.18)	571.24 (43.26)	36.72 (0.47)	624.36 (32.19)	51.90 (5.28)	855.31 (85.26)
p me guaiacol	N.D.	974.73 (74.54)	45.54 (0.00)	22.17 (0.10)	1289.93 (78.96)	12.21 (0.47)	585.19 (30.28)	34.81 (8.65)	580.96 (41.32)	57.19 (6.21)	1145.56 (5.99)
p eth guaiacol	N.D.	971.45 (60.82)	11.08 (5.92)	17.87 (0.01)	1263.65 (67.51)	7.74 (0.68)	589.06 (43.80)	27.73 (6.60)	465.66 (35.60)	41.15 (5.35)	1225.99 (59.49)
Total chemicals (mg/kg biomass)	113.21 (20.10)	9204.49 (298.78)	1193.22 (17.62)	538.12 (83.73)	9472.95 (245.29)	1602.98 (19.42)	8679.56 (181.03)	523.73 (17.84)	9594.84 (185.18)	788.79 (11.05)	13779.11 (800.72)

Cont-600 were compared using accelerated aging. The bio-oil found to be the most stable after accelerated aging was used to evaluate the influence of storage conditions because the aging reactions are not completely arrested after stepwise pyrolysis (as discussed in Section 3.3.1). The influence of accelerated aging on bio-oil is shown in Fig. 3, and the spectral information is provided in Figure S6.

The influence of temperature on bio-oil stability was assessed by adding AqBO to four air-tight glass bottles and storing them at 4 °C,

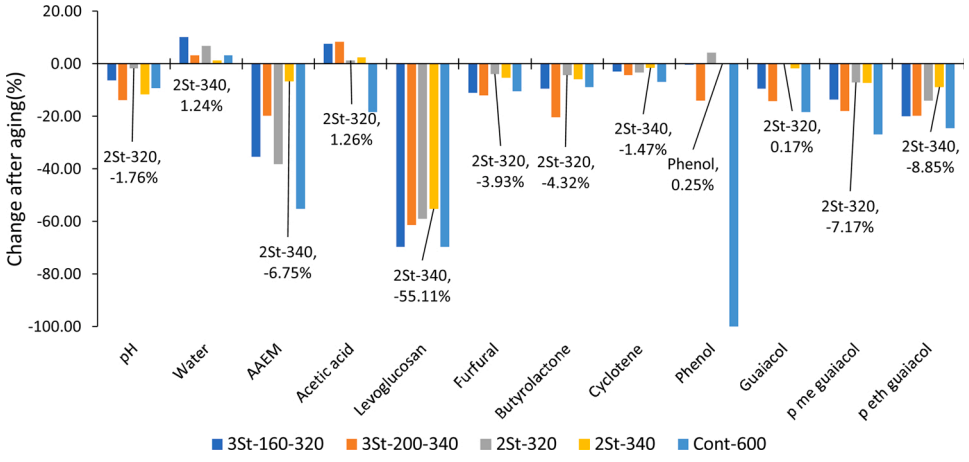

Fig. 3. Percentage change in bio-oil properties after accelerated aging for all pyrolysis cases.

20−25 °C, and 40 °C for four weeks. The influence of the solvents was assessed by adding AqBO to air-tight glass bottles and ultrapure water, methanol (>99.5 %), and ethanol (>99.5 %) to the bottles and storing the samples stored at 4 °C. AqBO was mixed with water at a ratio of 1:5 (v/v), with methanol and ethanol at a ratio of 1:0.5 (v/v) and 1:1 (v/v). The influence of increasing the bio-oil pH on its stability was evaluated by taking 5 g of AqBO and adding 25 % NaOH (aq) with magnetic stirring until the pH value reached 6. A fraction of the bio-oil was separated on neutralization, and the remaining neutralized aqueous bio-oil (Neu-AqBO) was stored at 4 °C for estimating the stability. The storage conditions have been labeled as water 1:5, pH neu, MeOH 0.5:1, MeOH 1:1, EtOH 0.5:1 and EtOH 1:1. The chemical composition of bio-oils stored without solvents was measured using GC/MS and HPLC as described in Section 2.3. However, the samples stored with solvents were diluted with methanol in a 1:10 ratio for GCMS analysis and 1:10 ultrapure water for HPLC analysis. The influence of aging parameters on bio-oil is shown in Figs. 4–7 and Figures S7-S12.

The bio-oil stability was evaluated using Eq. 6 to obtain the percentage change in the composition after accelerated aging and various storage conditions over four weeks.

$$\text{Percent change } (\%) = (P_{i,\text{ aged}} - P_{i,\text{ initial}}) \times 100/P_{i,\text{ initial}} \quad (6)$$

where, P_i is any bio-oil property, such as the chemical concentration (in mg/kg bio-oil), water content, pH, and AAEM concentration

3. Results and discussions

3.1. Pyrolysis product yields

Fig. 2 shows the pyrolysis products' yields obtained from each pyrolysis case, as listed in (Section 2.2). In all cases, the combined bio-oil yield from all steps was approximately 36–40 %. There was no significant difference in the yields of biochar, bio-oil, or pyrolysis gases between continuous and stepwise heating processes. The increase in the temperature during step 1 increased the bio-oil yield, leading to reduced bio-oil yield in the subsequent steps while keeping the total bio-oil yields constant. This was contrary to the results reported by Westerhof et al. [24] for the fast pyrolysis (≥1000 °C s^{-1}) of pinewood in a fluidized bed reactor; they reported a 3−6 wt% increase in char when the first step's temperature was between 320 °C and 340 °C, which was attributed to irreversible char-forming reactions. However, as shown in the next section, the current study's bio-oil composition was influenced by the temperature steps.

3.2. Bio-oil characterization

3.2.1. Physical and composition of bio-oil

Table 3 shows the bio-oil characterization from each pyrolysis case. The separation efficiency for these chemicals is provided in Table S2 to identify the most suitable temperatures for separating the oxygenated reactive groups.

In all cases, the bio-oil was primarily made up of water (Table 3). The water content in step 1 resulted from the vaporization (and subsequent condensation) of moisture in the biomass and in step 3 as a byproduct of condensation reactions, which tend to form high-molecular-weight compounds [11]. For the three-step heating, the water content was higher in steps 1 (80–82 %) and 3 (72–79 %) compared with step 2 (51–52 %). It was lower in step 1 (62–67 %) than step 2 (79–85 %) for the two-step heating. Further, because the temperature in step 1 increased from 320 °C to 340 °C, the water content increased. In comparing the stepwise cases with Cont-600, it can be seen that the water content as a byproduct of condensation reactions is reduced by increasing the number of steps. Hence, as the total chemical concentration is higher in Cont-600-derived bio-oil than in step 1 for the two-step pyrolysis and step 2 for three-step pyrolysis, the water content was also higher. The pH values in Table 3 show that the bio-oil fractions from step 1, in cases 2St-320 and 2St-340, and from steps 1 and 2, in cases 3St-160−320 and 3St-200−340, were acidic. However, the last fractions in all four cases were weakly alkaline. Further, with a decrease in the number of pyrolysis steps from three to one, the pH values increased. This trend resulted from a lower concentration of organic acids and a higher concentration of alkyl-substituted phenols (p-methyl guaiacol, p-ethyl guaiacol, isoeugenol), which reduced the acidity of the bio-oil fraction.

The influence of different temperatures on the bio-oil composition was also evident from the nine quantified chemicals' concentration and separation efficiencies. The thermal degradation of GNS began at 157 °C. Hence, in 3St-160−320, a low concentration of acetic acid and furfural was detected in step 1. As the temperature increased from 160 °C to 200 °C, in 3St-200−340, more acetic acid and furfural were separated in step 1. The highest concentration of all quantified chemicals was found in step 2. An increase in step 2 from 320 °C to 340 °C decreased acetic acid and levoglucosan concentration but increased the furfural concentration. All the phenolic compounds followed the expected trend; that is, the concentration in step 2 increased with increased temperature because of increased lignin availability. A comparison of the separation efficiency (Table S2) shows that 94–97 % of the nine quantified chemicals were concentrated in step 2 for three-step heating and 93–94 % in step 1 for two-step heating. The total chemicals concentrated in steps 1 and 3 accounted for 5–6 % of the total carboxyls, 3–4 % of the total anhydrosugars, 3–13 % of the total carbonyls, and 2–3 % of the total phenolics quantified in three-step heating. The chemicals concentrated in step 2 accounted for 4–9 % of the total carboxyls, 4–6 % of the total anhydrosugars, 7–9 % of the total carbonyls, and 7% of the total phenolics two-step heating.

Given these findings, it can be said that the concentrations in step 1

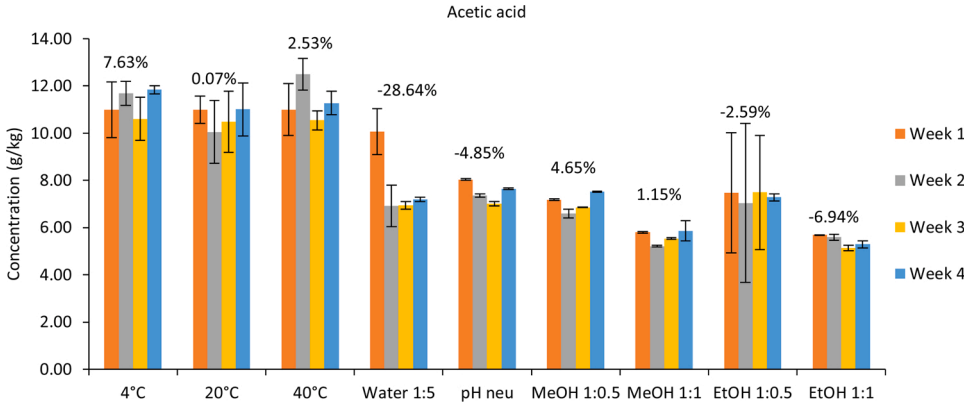

Fig. 4. Influence of storage conditions on change in concentration and total percentage change over four weeks for acetic acid in 2St-340 case.

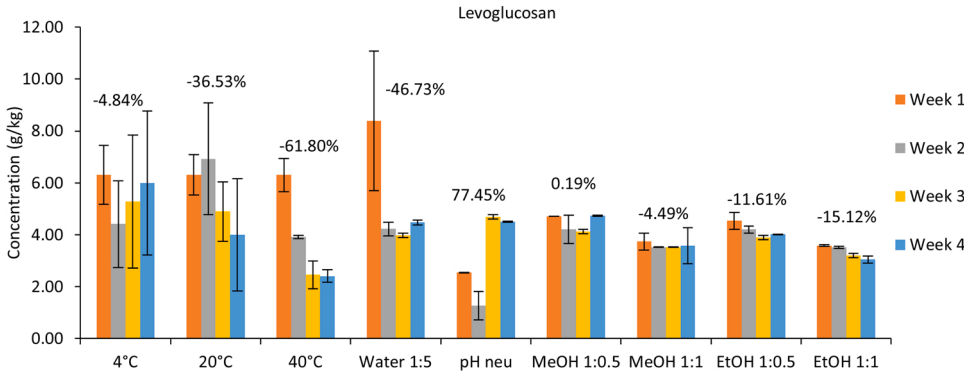

Fig. 5. Influence of storage conditions on change in concentration and total percentage change over four weeks for levoglucosan in 2St-340 case.

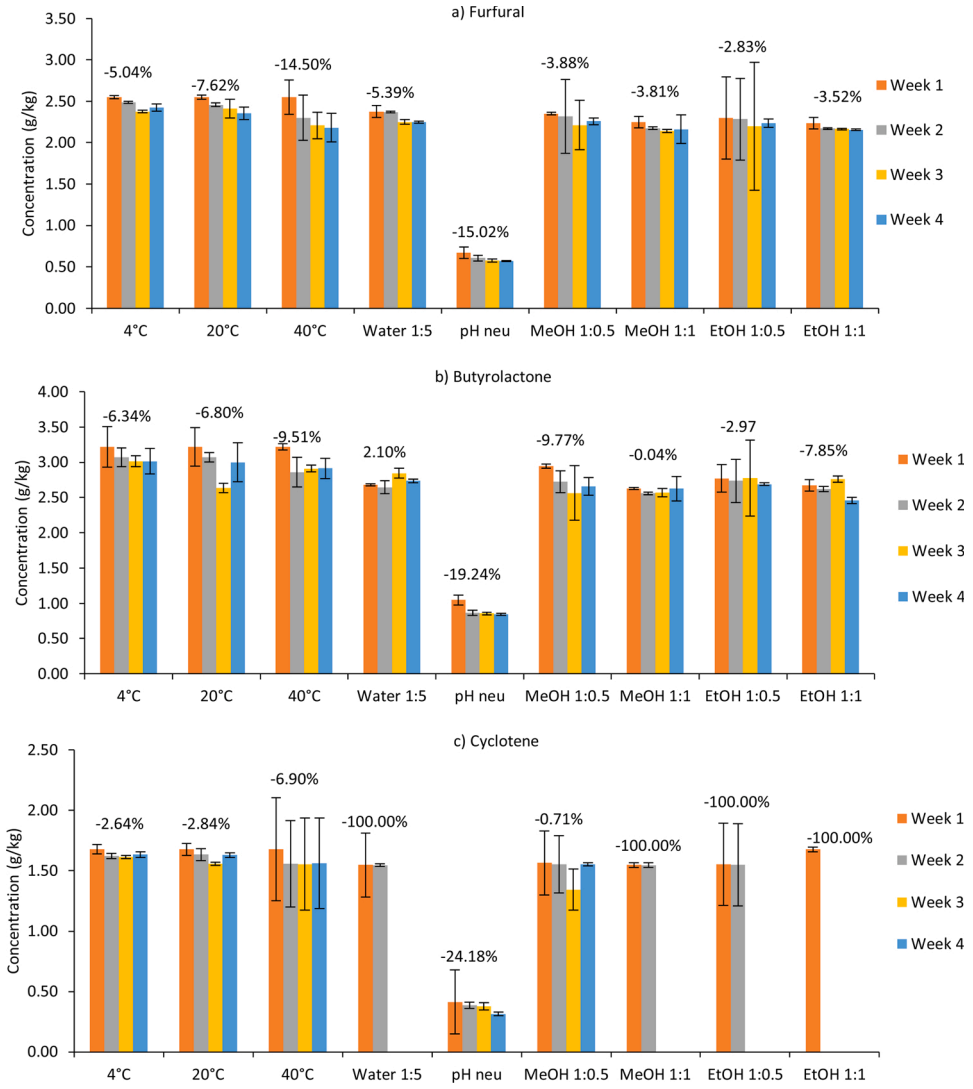

Fig. 6. Influence of storage conditions on change in concentration and total percentage change over four weeks for carbonyls (a) Furfural (b) Butyrolactone (c) cyclotene in 2St-340 case.

of the three-step heating were governed by hemicellulose breakdown only. In step 2, more cellulose and lignin are available for the production of levoglucosan and phenolic compounds. However, at a higher temperature, levoglucosan breaks down to form furfural as a byproduct, even though continued lignin breakdown hinders furfural formation [32]. The improvement in phenolic separation in two-step heating was because of a delayed thermal breakdown of lignin, particularly in the absence of an extra heating step. It appears that the three-step heating at 160 °C had the same influence as the drying of the biomass. Drying softens the lignin component and changes the pore structure of biomass (without altering the chemical structure), which improves the heat and mass transfer rates, hence contributing to better devolatilization [33].

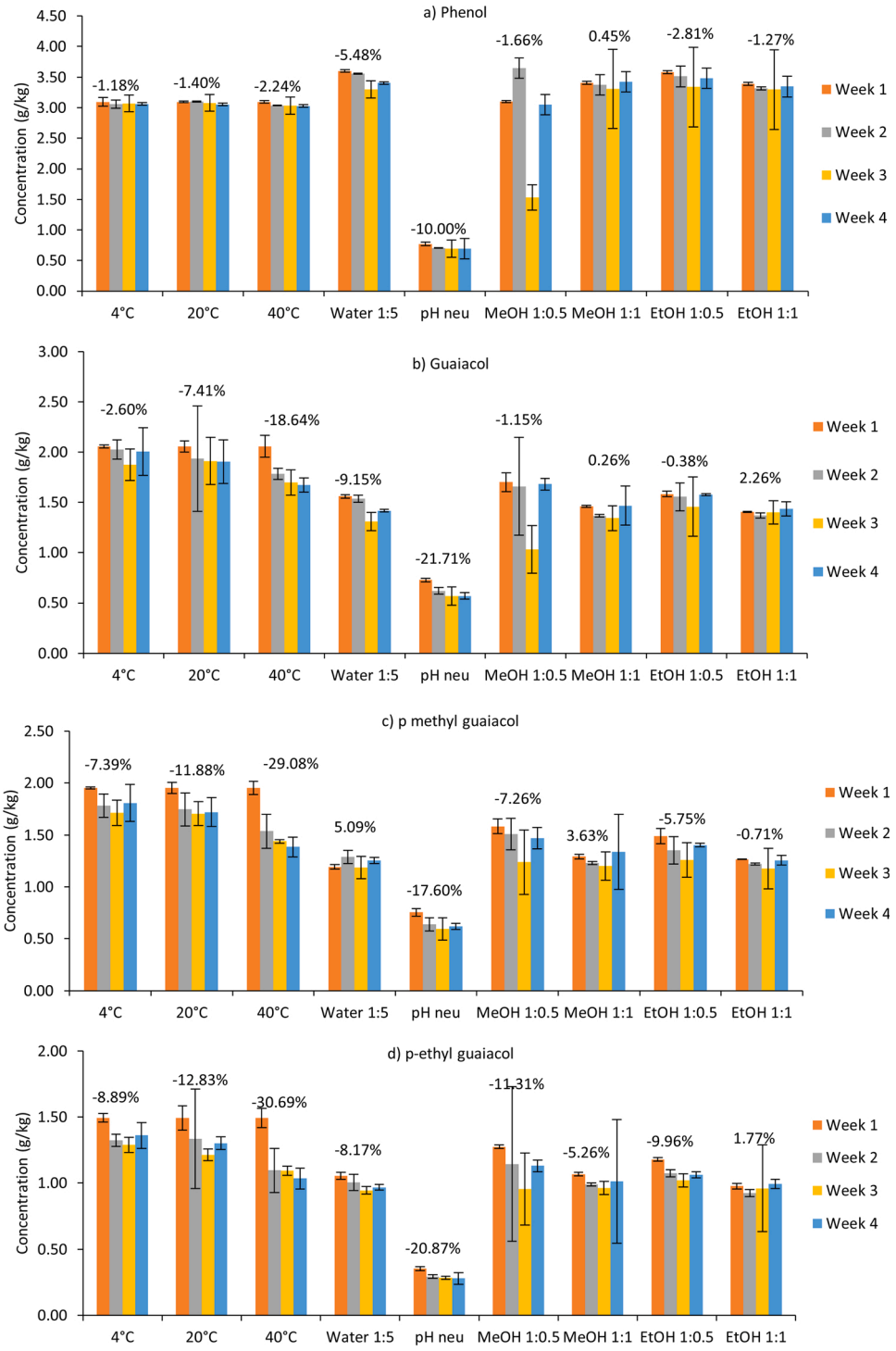

Fig. 7. Influence of storage conditions on change in concentration and total percentage change over four weeks for phenolics (a) phenol (b) guaiacol (c) p-methyl guaiacol (d) p-ethyl guaiacol in 2St-340 case.

In contrast, for the biomass, heating at 200 °C (3St-200−340) had the same influence as a torrefaction pre-treatment step for biomass [34]. A higher amount of hemicellulose content was converted in step 1, leading to increased cellulose and lignin availability for conversion in step 2. Table 3 also shows that the acetic acid yield and concentrations of most phenolics were higher in Cont-600. This helped to reduce the stability, as discussed in Section 3.3.

3.2.2. *Distribution of AAEMs in pyrolysis products*

The degree of transfer (%) of AAEMs from biomass to bio-oil (AqBO and NaqBO) and biochar produced from all five pyrolysis cases are reported in Table 4, along with the elemental mass balance closures. The concentration of AAEMs in pyrolysis products is given in Table S3. Although most AAEMs remained sequestered in the biochar during pyrolysis, 6.68–11.87 % of the AAEMs were transferred to the bio-oil. The total mass balance closures were between 60.29 % and 94.03 %, with the mass balance for Na being as low as 40.26 % and Mg being as high as 132.20 %. Other researchers also encountered these low balance closures for the inorganic elements because of the heterogeneity of biomass and pyrolysis products [35,36]. In considering the AAEMs individually,

Table 4
Degree of transfer (%) of AAEMs in bio-oil and overall mass balance closures.

Pyrolysis case		Na	K	Mg	Ca	Total mass balance
	Step 1	1.07	0.00	1.56	2.54	
	Step 2	10.90	6.62	3.39	7.36	
3St-160−320	Step 3	1.49	0.90	0.44	1.06	
	Bio-oil	13.46	7.52	5.39	10.95	9.63
	Biochar	27.69	54.01	72.12	61.62	50.66
	Balance	*54.61*	*69.05*	*82.90*	*83.53*	*60.29*
	Step 1	2.33	1.42	0.64	0.80	
	Step 2	7.43	4.45	2.18	3.06	
3St-200−340	Step 3	1.45	0.85	0.43	0.69	
	Bio-oil	11.21	6.72	3.25	4.55	7.04
	Biochar	29.05	56.77	81.77	63.27	53.26
	Balance	*51.47*	*70.22*	*88.28*	*72.37*	*60.29*
	Step 1	11.15	6.86	3.31	12.63	
	Step 2	2.41	1.45	0.96	2.96	
2St-320	Bio-oil	13.56	8.31	4.27	15.59	11.26
	Biochar	41.91	71.82	120.85	82.79	70.62
	Balance	*69.03*	*88.43*	*129.38*	*113.97*	*81.88*
	Step 1	8.20	5.13	2.27	3.59	
	Step 2	2.03	1.23	0.61	1.22	
2St-340	Bio-oil	10.22	6.36	2.88	4.81	6.68
	Biochar	48.11	94.13	129.32	103.00	87.35
	Balance	*68.56*	*106.85*	*135.08*	*112.63*	*94.03*
	Bio-oil	12.64	8.17	4.84	18.87	11.87
Cont-600	Biochar	77.69	121.94	85.73	77.04	77.04
	Balance	*90.33*	*130.11*	*90.57*	*95.91*	*88.92*

the transfer of the alkali metals Na and K to the bio-oil was 10.22–13.56 % and 6.36–8.31 %, respectively, while alkaline earth metals Mg and Ca were 2.88–5.39 % and 4.55–18.87 %, respectively. The differences in the degree of transfer of AAEMs were related to elemental speciation, nature of biomass, and pyrolysis temperature. Although both Na and K are monovalent, more Na than K was transferred. This was attributed to the interactions of the free radicals (H-radicals) generated during pyrolysis with the char-AAEM matrix through substitution reactions to releasing more Na [19]. Contrary to the reported trends [21,36], the transfer of Ca and Mg in the current study were higher than Na and K in all pyrolysis cases. This could be explained by comparing their concentrations in GNS (2.47 g/kg Mg and 9.26 g/kg Ca) with other biomasses since Ca and Mg transfer was dependent on the initial concentration in the biomass. At a concentration <1.00 g/kg (sugarcane bagasse), Ca and Mg were retained in biochar [21], but at a concentration of 2.00–3.95 g/kg (wheat straw and cow dung digestate), 1.00–5.00 % Ca, and Mg were transferred to the bio-oil [36]. The total transfer of AAEMs to all bio-oil fractions obtained from the different pyrolysis cases studied was in the order Cont-600 (11.87 %) > 2St-320 (11.26 %) > 3St-160−320 (9.63 %) > 3St-200−340 (7.04 %) > 2St-340 (6.68 %). Notably, the increase in the number of steps from two to three at the same temperature (2St-320 and 3St-160−320) led to a reduction in AAEMs transferred.

In contrast, an increase in the temperature from 320 °C to 340 °C (2St-340 and 3St-200−340) led to a decrease in AAEMs transferred. Based on previous studies [34,37], it can be speculated that an increase in the number of steps increased the secondary interaction of bio-oil vapors within the char-AAEM matrix, which leads to the re-adsorption of AAEM on biochar. Hence, the transfer of AAEMs was the highest in Cont-600 because of the absence of secondary interactions during pyrolysis. Further detailed analysis is required to explain these trends.

3.3. Bio-oil stability assessment

3.3.1. Changes in bio-oil composition after accelerated aging

The bio-oils obtained at different temperatures were compared using accelerated aging to identify the most suitable pyrolysis conditions of crop residues. The weight of the bio-oil samples was reduced by <2% after accelerated aging. The percentage change in the physical and chemical composition for the fresh and aged bio-oil samples is shown in Fig. 3. The pyrolysis case with the minimum change in properties is also shown in Fig. 3. The absolute concentrations of fresh and aged samples are provided in Table S4.

The pH decreased between 1.76 % and 13.80 % in all samples, with the minimum reduction observed for 2St-320. A decrease in pH was also reported in studies for the aging of bio-oil from other biomasses. It was caused by an increase in carboxyl compound concentration during the aging process [12,14,30]. Contrastingly, the water content increased by 1.24–10.11 % in all the bio-oil samples after aging because of condensation reactions during aging, where water is formed as a byproduct [30,38]. The maximum change in the AAEM concentrations occurred in Cont-600 (55.20 %), while the minimum was 2St-340 (6.75 %). However, in the current study, no correlation was found between the changes in concentration of AAEM and quantified chemicals, indicating that the elemental concentrations might not influence the bio-oil stability at the observed levels.

The percentage changes in the quantified chemicals in the fresh and aged bio-oil samples are shown in Fig. 3. The total percent change for all the nine quantified chemicals was the highest in continuous pyrolysis, followed by the three-step pyrolysis and two-step pyrolysis cases. Therefore, Cont-600 produced the least stable bio-oil compared with the stepwise heating cases. Looking at the chemicals individually, Fig. 3 shows that acetic acid concentration reduced in Cont-600 (18.45 %). However, it increased in all stepwise pyrolysis cases, with the minimum increase found in 2St-320 (1.26 %). Competing reactions involving the formation of carboxyls, such as the cracking of levoglucosan and consumption by esterification, are responsible for the overall change in carboxyl concentration during aging [12,14,30]. Thus, a decrease in acetic acid in Cont-600 shows that it is more rapidly consumed (clarify more). Levoglucosan decreased sharply after aging in all pyrolysis cases, with a minimum decrease in 2St-340 (55.11 %) and a maximum decrease in Cont-600 (69.68 %). This trend indicates that levoglucosan was an unstable compound under all pyrolysis conditions. The carbonyls and phenolic changes also show that the bio-oil obtained from two-step heating was more stable than three-step and continuous heating. Furthermore, when comparing the two-step heating cases, 2St-320 and 2St-340, it was evident that carbonyls were more stable at a higher temperature (2St-340), while phenolics were more stable at a lower temperature (2St-320). Therefore, the choice of temperature would depend on the final chemicals separated from the bio-oil, but exploring those separations was not in the current study's scope.

3.3.2. Influence of temperature and additives on the stability

Despite improved stability through stepwise heating, further stability improvements were explored for all quantified chemicals by comparing various storage temperatures (4 °C, 20−25 °C, and 40 °C) and additives (water, alkali, methanol, and ethanol) for the AqBO from step 1 in the 2St-340 case. The percentage change in each quantified chemical concentration over four weeks for each storage condition is also shown in Figs. 4–7. The weekly percentage change in the chemical concentrations is provided in Figure S12.

Some observations made during the analysis are listed here. First, adding various solvents and adjusting storage temperatures influenced the chemicals differently because of the differences in sensitivity to these conditions, making the analysis more complicated. Second, the aging reactions could be reduced but not entirely arrested by the storage conditions tested in the present study. Third, the lowest (4 °C) temperature was mostly preferable for the storage of chemicals. Fourth, the comparison of additives showed that dilution with water or increasing bio-oil pH played a minimal role in reducing bio-oil instability. There was a significant decrease in all chemicals after neutralization because of the loss of some bio-oil fraction after neutralization. Fifth, alcoholic additives have higher efficacy in preventing aging reactions in the bio-oil. Although methanol slowed down the aging of anhydrosugar and carbonyl compounds, ethanol was more effective for phenolics.

It was observed that acetic acid concentration increased when bio-oil was stored without additives. However, the fewest changes occurred at 20 °C (0.07 %). The reasons for the increase in acetic acid concentration are similar to those discussed in Section 3.3.1 for accelerated aging. The addition of solvents did not improve the stability of acetic acid any further. However, but the changes leveled off when ethanol (1:1) was used.

Levoglucosan followed an opposite trend to acetic acid, and after four weeks, its concentration reduced with increasing storage temperature. Storage at 40 °C caused a rapid breakdown, and the concentration reduced by 61.80 %. The decrease of levoglucosan with the addition of water and after neutralization reached up to 77.45 %. However, with methanol (0.5:1), the change was 0.19 %, indicating that methanol was very useful in stabilizing levoglucosan.

The changes in the concentration of all three carbonyls (furfural, butyrolactone, and cyclotene) are shown in Fig. 6 (a–c). The carbonyl concentrations were similar until the storage temperature was 20 °C or lower, but instability increased at a higher temperature. Furfural concentration changed the least (-2.83 %) when ethanol (0.5:1) was added to the bio-oil and stored at 4 °C. Previous studies have reported that a decrease in furfural through condensation reactions is compensated by its formation as a byproduct from levoglucosan breakdown [28,38]. However, a continued decrease in furfural over the four weeks (Fig. 6 a) indicates that condensation reactions were dominant. Like furfural, butyrolactone (Fig. 6 b) was the most stable when stored at 4 °C, but methanol (1:1) was a preferable additive. Fig. 6 c shows that cyclotene stability did not improve with alcohols, and it was not detected after the two weeks. Cyclotene concentrations were reduced, possibly because of the formation of acetals with alcohols [28]. The minimum change in cyclotene (2.64–2.84 %) occurred when stored without any additives and when the temperature was between 4 °C and 20 °C.

Fig. 7 (a–d) shows that the concentration fluctuation was less rapid in phenolics than the other quantified chemicals. This trend was explained by Meng et al. as being caused by the continuous fragmentation of lignin-derived phenolic oligomers into smaller molecules, which eventually undergo further condensation, leading to a final decrease in concentration [12]. The increase in storage temperatures influenced phenolics' stability in the order phenol > guaiacol > p-methyl guaiacol ≈ p-ethyl guaiacol. This could be because of the influence of aliphatic substituents on the hydroxyl group reactivity [39]. After four weeks, the concentration of phenol decreased by 2.24 % without additives and decreased by only 0.45 % with the addition of methanol (1:1). However, the other three phenolics decreased by 30 % when bio-oil was stored without additives. For guaiacol, the best storage condition was the addition of methanol (1:0.5). For p-methyl guaiacol and p-ethyl guaiacol, ethanol (1:1) was the most effective additive.

4. Conclusion

The influence of the stepwise pyrolysis was assessed in the current work through pyrolysis of groundnut shells using three-step, two-step, and continuous pyrolysis. The key conclusions to be drawn from this work are:

a) The reactive chemicals causing instability in bio-oil could be enriched in separate bio-oil fractions through stepwise pyrolysis
b) The differences in the degree of transfer of AAEMs were related to elemental speciation and pyrolysis temperature.
c) An increase in the number of steps reduced the transfer of AAEMs to bio-oil.
d) The bio-oil produced by two-step heating (step 1: 340 °C and step 2: 600 °C) was the most stable, and no correlation between AAEM concentration in this bio-oil and its stability was observed.
e) Four weeks of storage without solvents reduced anhydrosugars' concentration by 4.84 % at 4 °C, carbonyls by 5.06 %, and phenolics by 4.27 %.
f) Methanol addition further improved bio-oil stability, and the decrease in the concentrations of anhydrosugars and phenolics was <1% after four weeks at 4 °C.

CRediT authorship contribution statement

Anubhuti Bhatnagar: Conceptualization, Investigation, Methodology, Validation, Writing - original draft. **Robert Barthen:** Methodology, Validation, Writing - original draft. **Henrik Tolvanen:** Supervision, Writing - review & editing. **Jukka Konttinen:** Supervision, Writing - review & editing.

Declaration of Competing Interest

The authors declare that they have no known competing financial interests or personal relationships that could have appeared to influence the work reported in this paper.

Appendix A. Supplementary data

Supplementary material related to this article can be found, in the online version, at doi:https://doi.org/10.1016/j.jaap.2021.105219.

References

[1] J.J. Bozell, Renewable Feedstocks for Production of Chemicals, 2004.
[2] D. Mohan, U. Pittman Charles, P.H. Steele, Pyrolysis of wood/biomass for bio-oil: a critical review, Energy Fuels 20 (2006) 848–889, https://doi.org/10.1021/ef0502397.
[3] E. Cassou, Field burning (English), Agricultural Pollution 7 (2018). http://documents.worldbank.org/curated/en/989351521207797690/Field-Burning.
[4] W. Wang, Y. Liu, L. Zhang, The spatial distribution of cereal bioenergy potential in China, Gcb Bioenergy 5 (2013) 525–535, https://doi.org/10.1111/gcbb.12024.
[5] J. Yadav, B.R. Singh, Study on comparison of boiler efficiency using husk and coal as fuel in rice mill, SJPSET 2 (2011) 2229–7111. http://www.smslucknow.com/journals/vol2(2)/S2(2)-2011-01-16.pdf.
[6] S. Bhuvaneshwari, H. Hettiarachchi, J. Meegoda, Crop residue burning in India: policy challenges and potential solutions, Int. J. Environ. Res. Public Health 16 (2019) 832, https://doi.org/10.3390/ijerph16050832.
[7] P.A. Duc, P. Dharanipriya, B.K. Velmurugan, M. Shanmugavadivu, Groundnut shell -a beneficial bio-waste, Biocatal. Agric. Biotechnol. 20 (2019) 101206, https://doi.org/10.1016/j.bcab.2019.101206.
[8] S. Cheng, Z. Yuan, M. Anderson, M. Leitch, C. Xu, Synthesis of biobased phenolic resins/adhesives with methylolated wood-derived bio-oil, J. Appl. Polym. Sci. 126 (2012) E431–E441, https://doi.org/10.1002/app.35655.
[9] W. Li, L. Zhang, J. Peng, N. Li, X. Zhu, Preparation of high surface area activated carbons from tobacco stems with K2CO3 activation using microwave radiation, Ind. Crops Prod. 27 (2008) 341–347, https://doi.org/10.1016/j.indcrop.2007.11.011.
[10] A. Oasmaa, E. Kuoppala, Y. Solantausta, Fast Pyrolysis of Forestry Residue. 2. Physicochemical Composition of Product Liquid, Energy Fuels 17 (2003) 433–443, https://doi.org/10.1021/ef020206g.
[11] S. Czernik, D.K. Johnson, S. Black, Stability of wood fast pyrolysis oil, Biomass Bioenergy 7 (1994) 187–192, https://doi.org/10.1016/0961-9534(94)00058-2.
[12] J. Meng, A. Moore, D. Tilotta, S. Kelley, S. Park, Toward understanding of bio-oil aging: accelerated aging of bio-oil fractions, ACS Sustain. Chem. Eng. 2 (2014) 2011–2018, https://doi.org/10.1021/sc500223e.
[13] M. Cordella, C. Berrueco, F. Santarelli, N. Paterson, R. Kandiyoti, M. Millan, Yields and ageing of the liquids obtained by slow pyrolysis of sorghum, switchgrass and corn stalks, J. Anal. Appl. Pyrolysis 104 (2013) 316–324, https://doi.org/10.1016/J.JAAP.2013.07.001.
[14] J.V. Ortega, A.M. Renehan, M.W. Liberatore, A.M. Herring, Physical and chemical characteristics of aging pyrolysis oils produced from hardwood and softwood feedstocks, J. Anal, Appl. Pyrolysis. 91 (2011) 190–198, https://doi.org/10.1016/J.JAAP.2011.02.007.
[15] K.L. Kenney, W.A. Smith, G.L. Gresham, T.L. Westover, Understanding biomass feedstock variability, Biofuels. 4 (2013) 111–127, https://doi.org/10.4155/bfs.12.83.
[16] A. Oasmaa, Y. Solantausta, V. Arpiainen, E. Kuoppala, K. Sipilä, Fast pyrolysis bio-oils from wood and agricultural residues, Energy Fuels 24 (2010) 1380–1388, https://doi.org/10.1021/ef901107f.
[17] P.R. Patwardhan, J.A. Satrio, R.C. Brown, B.H. Shanks, Influence of inorganic salts on the primary pyrolysis products of cellulose, Bioresour. Technol. 101 (2010) 4646–4655, https://doi.org/10.1016/J.BIORTECH.2010.01.112.
[18] F.A. Agblevor, S. Besler, Inorganic Compounds in Biomass Feedstocks. 1. Effect on the Quality of Fast Pyrolysis Oils, Energy Fuels 10 (1996) 293–298, https://doi.org/10.1021/ef950202u.

[19] D.M. Keown, G. Favas, J. Hayashi, C.-Z. Li, Volatilisation of alkali and alkaline earth metallic species during the pyrolysis of biomass: differences between sugar cane bagasse and cane trash, Bioresour. Technol. 96 (2005) 1570–1577, https://doi.org/10.1016/J.BIORTECH.2004.12.014.
[20] D.M. Keown, J. Hayashi, C.-Z. Li, Effects of volatile–char interactions on the volatilisation of alkali and alkaline earth metallic species during the pyrolysis of biomass, Fuel 87 (2008) 1187–1194, https://doi.org/10.1016/j.fuel.2007.05.056.
[21] T. Okuno, N. Sonoyama, J. Hayashi, C.-Z. Li, C. Sathe, T. Chiba, Primary release of alkali and alkaline earth metallic species during the pyrolysis of pulverized biomass, Energy Fuels 19 (2005) 2164–2171, https://doi.org/10.1021/ef050002a.
[22] K. Yip, F. Tian, J. Hayashi, H. Wu, Effect of alkali and alkaline earth metallic species on biochar reactivity and syngas compositions during steam gasification, Energy Fuels 24 (2010) 173–181, https://doi.org/10.1021/ef900534n.
[23] P.J. de Wild, H. den Uil, J.H. Reith, J.H.A. Kiel, H.J. Heeres, Biomass valorisation by staged degasification: a new pyrolysis-based thermochemical conversion option to produce value-added chemicals from lignocellulosic biomass, J. Anal. Appl. Pyrolysis 85 (2009) 124–133, https://doi.org/10.1016/J.JAAP.2008.08.008.
[24] R.J.M. Westerhof, D.W.F. Brilman, M. Garcia-Perez, Z. Wang, S.R.G. Oudenhoven, S.R.A. Kersten, Stepwise fast pyrolysis of pine wood, Energy Fuels 26 (2012) 7263–7273, https://doi.org/10.1021/ef301319t.
[25] A. Bhatnagar, H. Tolvanen, J. Konttinen, Potential of stepwise pyrolysis for on-site treatment of agro-residues and enrichment of value-added chemicals, Waste Manag. 118 (2020) 667–676, https://doi.org/10.1016/j.wasman.2020.09.022.
[26] A. Oasmaa, I. Fonts, M.R. Pelaez-Samaniego, M.E. Garcia-Perez, M. Garcia-Perez, Pyrolysis oil multiphase behavior and phase stability: a review, Energy Fuels 30 (2016) 6179–6200, https://doi.org/10.1021/acs.energyfuels.6b01287.
[27] J.P. Diebold, S. Czernik, Additives to lower and stabilize the viscosity of pyrolysis oils during storage, Energy Fuels 11 (1997) 1081–1091, https://doi.org/10.1021/ef9700339.
[28] S. Ren, X.P. Ye, Stability of crude bio-oil and its water-extracted fractions, J. Anal. Appl. Pyrolysis 132 (2018) 151–162, https://doi.org/10.1016/j.jaap.2018.03.005.
[29] L.K.-E. Park, S. Ren, S. Yiacoumi, X.P. Ye, A.P. Borole, C. Tsouris, pH neutralization of aqueous bio-oil from switchgrass intermediate pyrolysis using process intensification devices, Energy Fuels 31 (2017) 9455–9464, https://doi.org/10.1021/acs.energyfuels.7b00854.
[30] A. Oasmaa, E. Kuoppala, Fast Pyrolysis of Forestry Residue. 3. Storage Stability of Liquid Fuel, Energy Fuels 17 (2003) 1075–1084, https://doi.org/10.1021/ef030011o.
[31] S. Black, J.R. Ferrell, Accelerated aging of fast pyrolysis bio-oil: a new method based on carbonyl titration, RSC Adv. 10 (2020) 10046–10054, https://doi.org/10.1039/D0RA00046A.
[32] X. Wang, Y. Liu, X. Cui, J. Xiao, G. Lin, Y. Chen, H. Yang, H. Chen, Production of furfural and levoglucosan from typical agricultural wastes via pyrolysis coupled with hydrothermal conversion: influence of temperature and raw materials, Waste Manag. 114 (2020) 43–52, https://doi.org/10.1016/j.wasman.2020.06.045.
[33] D. Chen, D. Li, X. Zhu, Effect of moisture content on the devolatilization and kinetics of corn straw, energy sources, part a recover, Util. Environ. Eff. 37 (2015) 1005–1011, https://doi.org/10.1080/15567036.2011.596904.
[34] Q. Dong, S. Zhang, K. Ding, S. Zhu, H. Zhang, X. Liu, Pyrolysis behavior of raw/torrefied rice straw after different demineralization processes, Biomass Bioenergy 119 (2018) 229–236, https://doi.org/10.1016/j.biombioe.2018.09.032.
[35] N. Jendoubi, F. Broust, J.M. Commandre, G. Mauviel, M. Sardin, J. Lédé, Inorganics distribution in bio oils and char produced by biomass fast pyrolysis: the key role of aerosols, J. Anal. Appl. Pyrolysis 92 (2011) 59–67, https://doi.org/10.1016/j.jaap.2011.04.007.
[36] E.J. Leijenhorst, W. Wolters, L. van de Beld, W. Prins, Inorganic element transfer from biomass to fast pyrolysis oil: Review and experiments, Fuel Process. Technol. 149 (2016) 96–111, https://doi.org/10.1016/j.fuproc.2016.03.026.
[37] H. Chen, X. Chen, Z. Qiao, H. Liu, Release and transformation characteristics of K and Cl during straw torrefaction and mild pyrolysis, Fuel 167 (2016) 31–39, https://doi.org/10.1016/j.fuel.2015.11.059.
[38] R.N. Hilten, K.C. Das, Comparison of three accelerated aging procedures to assess bio-oil stability, Fuel 89 (2010) 2741–2749, https://doi.org/10.1016/j.fuel.2010.03.033.
[39] R. Fahmi, A.V. Bridgwater, I. Donnison, N. Yates, J.M. Jones, The effect of lignin and inorganic species in biomass on pyrolysis oil yields, quality and stability, Fuel 87 (2008) 1230–1240, https://doi.org/10.1016/J.FUEL.2007.07.026.